

Microstructural characterization and *in vitro* bioactivity of SrO-SiO₂-Na₂O-CaO-B₂O₃-P₂O₅ glassesRawhia L. Elwan ^{a,b,*}, Mona R. Al-Shathly ^c^a Chemistry Department, Faculty of Science for Girls in Ar'ar, Northern Border University, Kingdom of Saudi Arabia^b Glass Research Department, National Research Centre (NRC), El-Behoos Str., Dokki, 12622 Cairo, Egypt^c Biology Department, Science Faculty for Girls, King Abdulaziz University, Jeddah, Kingdom of Saudi Arabia* Corresponding author: r.lotfy2000@hotmail.com

Abstract: SrO-SiO₂-Na₂O-CaO-B₂O₃-P₂O₅ glasses have been prepared using the conventional melting and annealing method. B₂O₃ content was systematically increased from 0 to 20 mol%, at the expense of P₂O₅, in the chemical composition of these glasses. Density and Vickers microhardness of the prepared glasses were measured. *In vitro* bioactivity of these glasses was assessed by soaking in the simulated body fluid (SBF) at 37 ± 0.5 °C for 7, 14 and 30 days. The structure and composition of the solid reaction products were characterized using X-ray diffraction (XRD), Fourier transform infrared spectroscopy (FTIR) and scanning electron microscopy (SEM) coupled with energy dispersive spectroscopy (EDS). The variation of ion concentrations in the SBF solution after soaking was detected by means of inductive coupled plasma-atomic emission spectroscopy (ICP-AES). The obtained results showed the formation of a bioactive hydroxyapatite (HA) layer on the surface of glasses after the *in vitro* assays. In a collective view of the obtained results, it can be concluded that increasing B₂O₃ content in the present glass composition enhances the bioactivity of the glasses. Based on the change in chemistry of the SBF, phase contents and the evaluation of Ca-P layer growth, a mechanism has been suggested for the evolution and growth of HA layer on glass surfaces immersed in SBF. The bone-like apatite formation of glass surface suggests the potential of the studied glasses for integration with bone.

[Rawhia L. Elwan, Mona R. Al-Shathly. **Microstructural characterization and *in vitro* bioactivity of SrO-SiO₂-Na₂O-CaO-B₂O₃-P₂O₅ glasses.** *Life Sci J* 2014;11(12s):36-46]. (ISSN: 1097-8135). <http://www.lifesciencesite.com>. 7

Keywords: Bioactivity; Boro-phosphate glass; FTIR; SEM-EDAX; XRD

1. Introduction

Over the past several years, research in the field of biomaterials has advanced notably, developing different technological processes and materials for medical applications, Aguiar et al., (2008). Variety of bioactive glasses, glass ceramics and calcium phosphate based glasses are used for biomedical applications such as dental, orthopedic and maxillofacial fields. In particular, a bioactive calcium phosphate based implant forms, after integration with bone, a biologically active hydroxycarbonate apatite (HCA) layer at the bone-implant interface which favors bonding with bone and soft tissues, Marikani et al., (2008). The first bioactive glass, 45S5 bioglass (45 wt% SiO₂, 24.5CaO, 6P₂O₅, and 24.5Na₂O), was developed by Hench and co-workers, Hench et al., (1971) It is one of the most studied and well characterized bioglass materials. After this, several bioglass materials were prepared and extensively studied by researchers all-over the world. It is now widely accepted that for establishing bond with bone, such biologically active apatite surface layer must form at the material-bone interface. The development of these bioactive apatite layers is the common characteristic of all known inorganic materials used for orthopedic implants, bone replacement and bone

tissue engineering scaffold, (Ducheyne 1985; Hench, 1998; Rezwani et al., 2006) Bioactive glasses have attracted the attention of researchers due to their ability to react with the physiological environment by forming durable and mechanically strong bonds across the biological tissue-glass interface. This property is intimately related to the open structure of the glasses, which is responsible for selective dissolution in physiological environments. The incorporation of certain network modifier cations (such as Na⁺, K⁺, Mg²⁺, Ca²⁺, etc.) disrupts the glassy network, leading to the structure depolymerization and the formation of non-bridging oxygen atoms (NBO), also named terminal oxygens (O_T) Aguiar et al., (2008).

The silica based bioactive materials have shown great success in many clinical applications in both dental and orthopedic field, but due to its insoluble properties, it has potential as long-term device. But, the use of phosphate glasses offers a more controlled rate of dissolution, as compared to silica containing glasses. The development of phosphate glasses for use in orthopedic implants has attracted much interest due to their chemical and physical properties. Therefore, SiO₂ free glass compounds are also attempted for bioglass implantations. Phosphate

based glasses proved to be simple, easier to be produced, biodegradable and biocompatible with many human connective tissue cells. In addition, phosphate based glasses seem to be used as bioresorbable materials because of their solubility. These degradable and absorbable glasses, by the human body, are useful as suture thread in bone fracture fixation applications, as dental implants and as carriers in drug delivery Marikani et al., (2008). Furthermore, recent data, (Richard2000; Day, 2003; Yao et al., 2007; Ning et al., 2007; Han et al., 2008; Fu et al., 2010) have demonstrated that silica-free borate glasses also exhibit bioactive behavior. A borate glass, with the same composition as 45S5 glass but with all the SiO₂ content replaced by B₂O₃, was investigated by Richard (2000), who found that the HA layer formed more rapidly on the borate glass than on 45S5 glass. CaO-containing alkali-borate glasses with special compositions in the systems Li₂O-CaO-B₂O₃ and Na₂O-CaO-B₂O₃ have been observed to convert rapidly to HA when placed in an aqueous phosphate solution (0.25 M K₂HPO₄) at 37°C (the body temperature). Porous or hollow HA microspheres prepared by this route have a mesoporous structure of nanosized particles and high surface area of 100-200 m²/g. As such, the glass conversion method provides another route for the production of biologically active HA materials and devices for biomedical applications (Day, 2003; Yao et al., 2007; Ning et al., 2007; Han et al., 2008; Fu et al., 2010).

The conversion of a bioactive glass (or glass-ceramic) to HA in vitro, when immersed in an aqueous phosphate solution such as the SBF, provides a measure of its bioactive potential in vivo. Therefore, it is important to understand the factors that influence the conversion of bioactive glass to HA in vitro, Ducheyne and Qiu (1999). Therefore, the objective of this work was to study the in vitro bioactivity of SrO-SiO₂-Na₂O-CaO-B₂O₃-P₂O₅ glasses utilizing a combination of analytical tools

2. Materials and experimental procedures

2.1. Materials

2.1.1. The starting materials:

They were powders of analytical reagent grade of SrO, SiO₂, Na₂CO₃, CaCO₃, H₃BO₃ and NH₄H₂PO₄, respectively. They were well mixed powders containing appropriate amounts of the raw materials

2.2. Methods:

2.2.1. Glass preparation

Glasses, having the chemical composition of 5SrO-10SiO₂-20Na₂O-5CaO-xB₂O₃-(60-x)P₂O₅, where x= 0, 5, 10, 15 and 20 mol%, have been

prepared using the conventional melting and annealing method.

The starting materials were melted in a platinum crucible in an electric furnace at 1200-1250 °C for 1 h in air. The molten liquid was occasionally stirred to ensure homogeneous mixing of all constituents and to obtain bubble-free samples. The glass, formed by quenching the melt on a stainless-steel mold, was immediately transferred to another muffle furnace where it was annealed at about 380°C for 1 h. Then, the muffle was switched off and the temperature decreased to room temperature with a rate of 25°C/h. In samples containing 15 and 20 mol% B₂O₃, partial devitrification occurred during pouring of these samples. Grinding of the devitrified product and its remelting yielded transparent colorless glasses. The nominal compositions of the prepared glasses together with their abbreviations are shown in Table (1).

The prepared glass specimens were cut and polished into cubes of dimensions 5x5x5 mm for in vitro bioactivity evaluation.

2.2.2. Density and hardness measurements

The density (ρ) of each glass sample was measured at room temperature using Archimedes method with water as the immersion liquid. The density was calculated according to the following formula:

$$\rho = [(W_{\text{air}})/(W_{\text{air}} - W_{\text{water}})] \cdot [\rho_{\text{water}}] \quad (1)$$

where:

- W_{air} and W_{water} are the weight of glass sample in air and in water, respectively,
- ρ_{water} is the density of water.

Vickers microhardness (H_V) of the 2 mm thick polished samples was measured with a Shimadzu-HMV (Japan) microhardness tester using 100 g load under ambient laboratory conditions with a constant indenter dwell time of 15 s. At least five indentations were measured for each data point. The indentation was made using a square based pyramidal diamond with face angle 136° with measuring microscope and video monitor. The hardness was calculated using Eq. (2), by finding the ratio of the applied load to the pyramidal contact area of the indentation:

$$H_V = 1.854 P / D^2 \quad (2)$$

Where:

- P is the applied indentation load and
- D is the measured indentation diagonal.

2.2.3. In vitro bioactivity evaluation

In vitro bioactivity was assessed by soaking the polished glass samples in the simulated body fluid (SBF) prepared according to the recipe proposed by (Kokubo et al. 1999; Kokubo and Takadama, 2006) mentioned in many other published articles, for instance, (Aguiar et al., 2008; Salman et al., 2012; Renghini et al., 2013). SBF is a cellular aqueous

solution with inorganic ion composition almost equal to human blood plasma. In the typical preparation, SBF solution was prepared by mixing the appropriate amounts of sodium chloride, sodium bicarbonate, potassium chloride, calcium chloride, dibasic potassium phosphate and magnesium chloride in deionized water with the help of magnetic stirrer in a beaker, according to the concentrations given in (Kokubo *et al.* 1999; Kokubo and Takadama, 2006 Aguiar *et al.*, 2008; Salman *et al.*, 2012; Renghini *et al.*, 2013). Initially, glass samples were washed ultrasonically in acetone for a few minutes and left to dry in air. Then, the samples were placed in polyethylene bottles containing 50 ml of SBF solution. The bottles were kept in an incubator maintained at $37 \pm 0.5^\circ\text{C}$ (human body temperature) for 7, 14 and 30 days. In a recent work, Siqueira and Zanotto (2013) suggested another experimental parameter which additionally describes the immersion circumstances. This parameter is the sample mass to SBF solution volume ratio. In the present experiments, this ratio is $0.007\text{--}0.008 \text{ g (ml)}^{-1}$. This means the use of excess SBF volume surrounding the glass samples. After each specified time interval, samples were removed from the SBF and dried at room temperature. The surfaces of dried samples (before and after soaking) were analyzed by XRD, FTIR and SEM-EDAX to examine the formation of HCA layer. On the other hand, the variation of ion concentrations in the SBF solution after soaking was detected by means of inductive coupled plasma-atomic emission spectroscopy (ICP-AES).

XRD analysis was used to ensure the amorphous structure of the as-prepared glasses as well as to identify whether crystalline phases have

been developed on their surfaces after soaking in SBF. XRD patterns were recorded using Bruker AXS D8 Advance X-ray diffractometer (40 kV, 20 mA) from 5° to 70° in steps of 0.01° . The $\text{Cu K}\alpha$ radiation with Ni filtered is used for X-ray analysis. The reference data for the interpretation of the XRD patterns were obtained from JCPDS X-ray diffraction card files.

Glass surfaces before and after immersion in the SBF were examined using Fourier transform infrared spectroscopy (FTIR spectrophotometer type Jasco-300E, Japan). FTIR spectra were collected in diffuse reflectance mode directly on the sample surface (400 scans, resolution at 2 cm^{-1}) in the wave number region of $2000\text{--}400 \text{ cm}^{-1}$.

Before and after in vitro tests in SBF, the microstructure of glass surfaces was studied using a scanning electron microscope equipped with energy dispersive X-ray analysis (SEM-EDAX, type Inspect S, T810, D8571, FEI Co., Japan) with accelerating voltage of 30 kV and magnification 10x up to 300 000x. Energy dispersive spectroscopy (EDS) was used to investigate the compositional modification occurred on glass surfaces after soaking in SBF.

3. Results

The measured values of density and Vickers microhardness are listed in Table (1). Density decreases slightly from 3.265 to 2.643 g cm^{-3} , while hardness increases gradually from 334 to 392 kg mm^{-2} with increasing B_2O_3 content. XRD patterns of all the as-prepared glasses showed no identifiable diffraction peaks that result from lattice periodicity confirming the amorphous structure of the prepared glass series.

Table 1. Nominal composition, density and Vickers microhardness of the studied glasses.

Glass code	Chemical composition (mol%)						Density (ρ) (g cm^{-3}) ± 0.001	Vickers microhardness (H_v) (kg mm^{-2}) ± 3
	SrO	SiO ₂	Na ₂ O	CaO	B ₂ O ₃	P ₂ O ₅		
GB0	5	10	20	5	--	60	3.265	334
GB5	5	10	20	5	5	55	3.155	357
GB10	5	10	20	5	10	50	2.922	369
GB15	5	10	20	5	15	45	2.876	375
GB20	5	10	20	5	20	40	2.643	392

Fig. (1a) gave the XRD pattern of the as-prepared glass GB20 as a representative sample. Additionally, Fig. (1b-d) showed the X-ray diffractograms of the same glass after soaking in SBF for 7, 14 and 30 days in which diffraction peaks corresponding to that of a standard crystalline HA ($\text{Ca}_{10}(\text{PO}_4)_6(\text{OH})_2$), JCPDS 72-1243, can be observed indicating the formation of HA on the glass surface during the reaction after 14 and 30 days; as shown in

Fig. (1c) and (1d), respectively. The intensity of peaks became higher after immersion in SBF for 30 days, as shown in Fig. (1d).

These peaks were not found in the XRD pattern of this glass (GB20) after soaking for 7 days, as depicted in Fig. (1b), and the 2θ -position of the recorded broad halo may suggest the formation of an amorphous HA or very poorly crystallized HA or a combination of both. Similar XRD behavior was

exhibited by the other four glass compositions. To avoid repetition, only XRD patterns of glass GB20 were given.

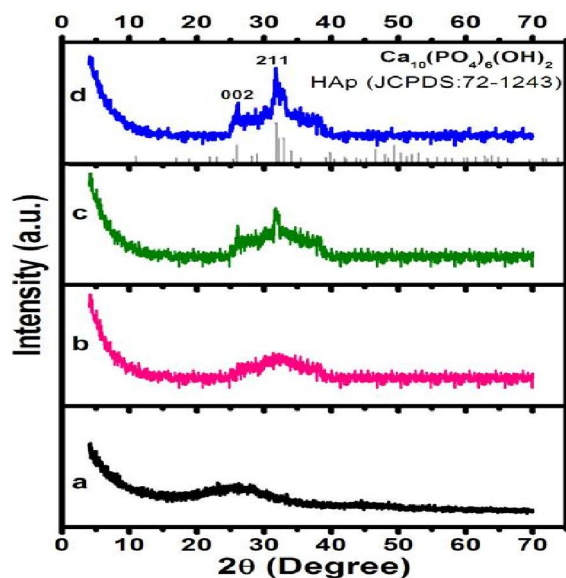
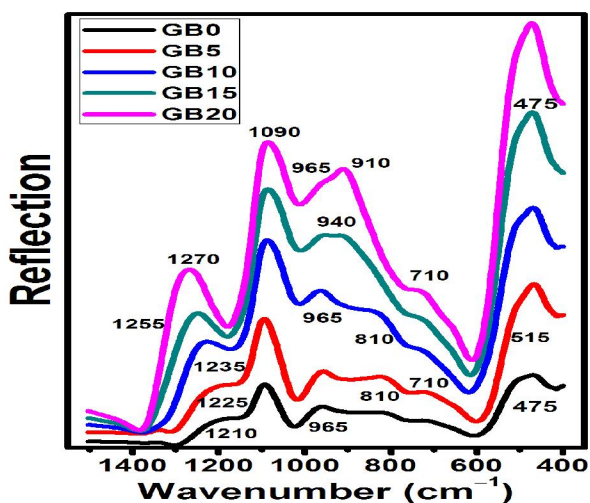


Fig. (1) XRD patterns of glass GB20: a) as-prepared sample; b-d) after soaking the glass in SBF for 7, 14 and 30 days, respectively

FTIR reflection spectra of the as-prepared glasses (GB0-GB20), i. e. before soaking in the SBF solution, are shown in Fig. 2.

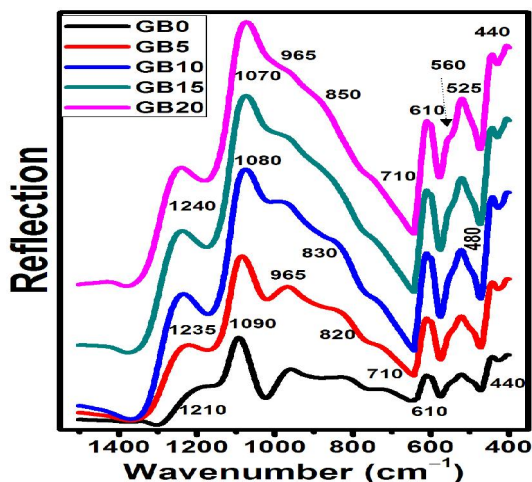


Fig(2): FTIR spectra of the as-prepared glasses, i. e. before soaking in the SBF.

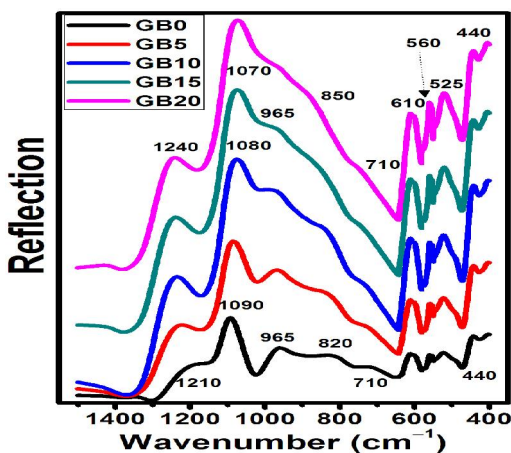
These spectra indicated the structural changes in the studied glasses resulting from the compositional variation. A set of IR bands appeared in the spectra of all glasses. These bands were: a strong broad band centered at 475 cm^{-1} with a shoulder at about 515 cm^{-1} , a broad shoulder at about 710 cm^{-1} and an

intense broad band centered at 1090 cm^{-1} . Additionally, a broad shoulder was recorded at about 810 cm^{-1} in the spectra of glasses GB0, GB5 and GB10. This shoulder might be combined in the broadness of the two broad bands located at about 940 and 910 cm^{-1} in the spectra of glasses GB15 and GB20, respectively. A medium broad band was also recorded at about 965 cm^{-1} in the spectra of glasses GB0, GB5 and GB10. This band appeared as a shoulder at the same wave number, i. e. 965 cm^{-1} , in the spectra of glasses GB15 and GB20. The broad shoulder recorded at 1210 cm^{-1} in the spectrum of glass GB0 becomes broader and shifted to 1225 cm^{-1} in the spectrum of glass GB5. It turned into a medium broad band which is shifted to 1235 , 1255 and 1270 cm^{-1} in the spectra of glasses GB10, GB15 and GB20, respectively. It can be observed that the intensity of this band successively increases with the gradual increase of B_2O_3 content in the glass composition from 10 to 20 mol%. Inspection of the relative intensities of bands recorded in the same spectrum indicates that, in the spectra of all glasses, the band located at 475 cm^{-1} with its shoulder at 515 cm^{-1} are more intense than that located at 1090 cm^{-1} . Figs. (3-5) showed the reflection IR spectra of glass surfaces after soaking in the SBF for 7, 14 and 30 days, respectively. In comparison, these spectra were markedly different from those of the as-prepared glasses. After 7 days, as shown in Fig. (3), all the spectra revealed IR vibration bands at 440 , 525 and 610 cm^{-1} ; and shoulders at 480 , 560 and 710 cm^{-1} . Additional vibrations included a broad shoulder at 820 cm^{-1} in the spectra of glasses GB0 and GB5 which is shifted to 830 cm^{-1} in the spectra of glasses GB10 and GB15, and to 850 cm^{-1} in the spectrum of glass GB20. The medium broad peak observed at 965 cm^{-1} in the spectra of glasses GB0 and GB5 turned into a broad shoulder at the same wave number in the spectra of glasses GB10, GB15 and GB20. The intense broad band recorded at 1090 cm^{-1} in the spectra of glasses GB0 and GB5 was shifted to 1080 cm^{-1} in the spectra of glasses GB10 and GB15, and to 1070 cm^{-1} in the spectrum of glass GB20. Similarly, the broad shoulder located at 1210 cm^{-1} in the spectrum of glass GB0 turned into a medium broad band of successively increased intensity in the same order and is shifted gradually to 1240 cm^{-1} .

After 14 days, FTIR spectra of the studied glasses, presented in Fig. (4), show quite similar vibration bands to those obtained after 7 days, except only one difference which is the change of the shoulder recorded at 560 cm^{-1} into a relatively weak band at the same wave number in the spectra of all studied glasses.



Fig(3): FTIR spectra of the investigated glasses after soaking in the SBF for 7 days.

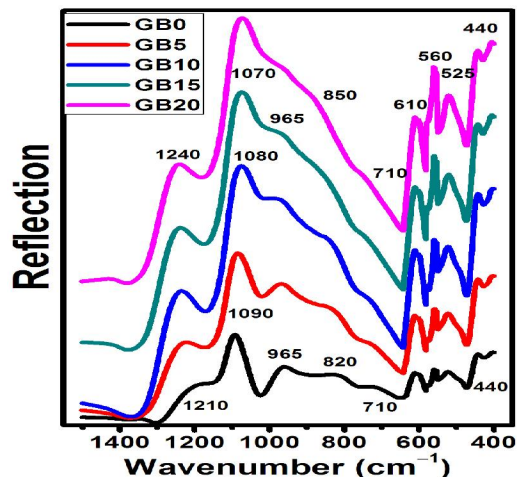


Fig(4): FTIR spectra of the studied glasses after soaking in the SBF for 14 days.

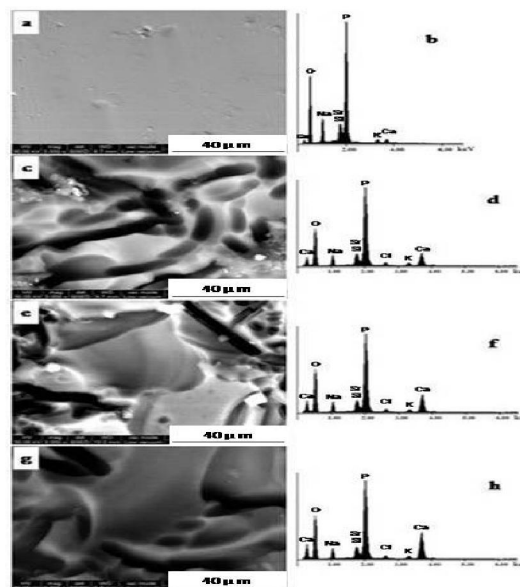
After 30 days, the intensity of this band successively increases with increasing B_2O_3 content in the glass composition reaching a maximum in the spectrum of glass GB20, as seen in Fig. (5), keeping all other vibration bands exhibited by the glasses after 14 days. In contrast to the situation before soaking in the SBF, the band at $1090-1070\text{ cm}^{-1}$ becomes more intense than the bands and shoulders in the range $610-440\text{ cm}^{-1}$ in the spectra of all glasses after soaking for 7, 14 and 30 days.

Figs. (6-10) showed the SEM micrographs and the corresponding EDX spectra of the studied glasses (GB0-GB20) before and after soaking in the SBF. SEM images of the reacted glass-surfaces showed marked changes in the microstructure when compared to that of the starting glasses. In general, the smooth surface typical of a dense glass changed to a porous particulate surface after immersion in the SBF solution. It can be seen, from these micrographs, that cracked HA layer was formed on glass-surfaces

after 7 days. Gradual increase in the compactness of this layer could be noticed with increasing immersion time to 14 and 30 days such that fairly compact and dense apatite layer was formed after 30 days. EDS spectra support these observations where a considerable increase in the ratio of relative intensities of Ca: P peaks could be obviously noticed with increasing of the immersion time. This indicates the increase of compositional Ca: P ratio in the formed layer following the stoichiometric HA, $(Ca_{10}(PO_4)_6(OH)_2)$, ratio.



Fig(5): FTIR spectra of the investigated glasses after soaking in the SBF for 30 days.



Fig(6): SEM micrographs and the corresponding EDX spectra of glass GB0: a, b) as-prepared glass, i. e. before immersion in the SBF; c, d) after immersion in the SBF for 7 days; e, f) after immersion in the SBF for 14 days; g, h) after immersion in the SBF for 30 days.

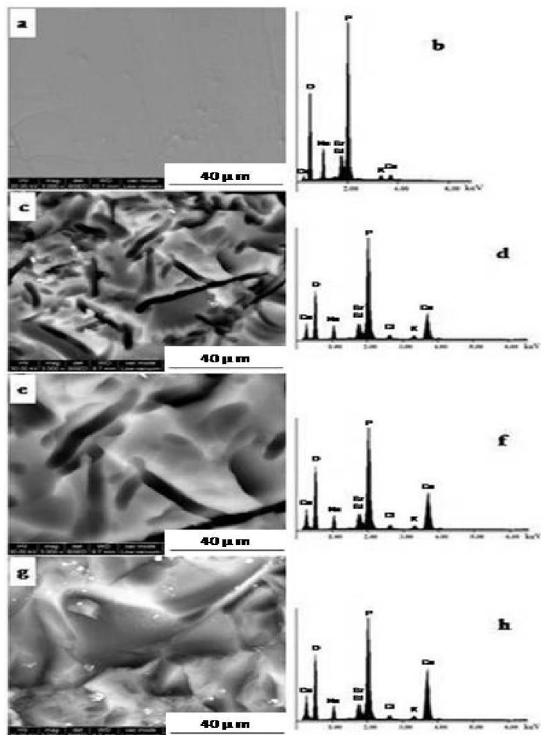


Fig (7): SEM images and the corresponding EDAX spectra of glass GB5: a, b) as-prepared glass, i. e. before immersion in the SBF; c, d) after immersion in the SBF for 7 days; e, f) after immersion in the SBF for 14 days; g, h) after immersion in the SBF for 30 days.

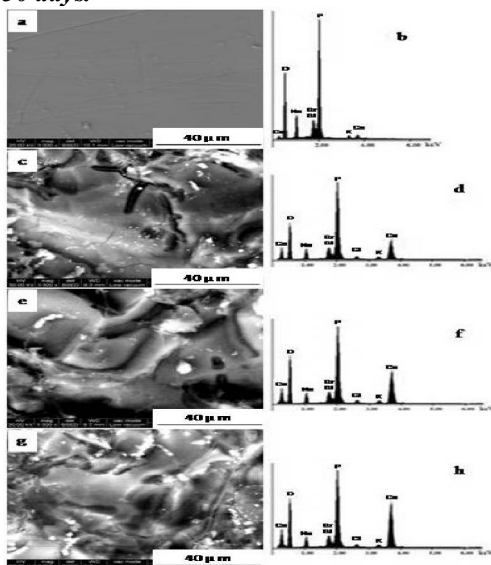


Fig (8): SEM micrographs and the corresponding EDAX spectra of glass GB10: a, b) as-prepared glass, i. e. before immersion in the SBF; c, d) after immersion in the SBF for 7 days; e, f) after immersion in the SBF for 14 days; g, h) after immersion in the SBF for 30 days.

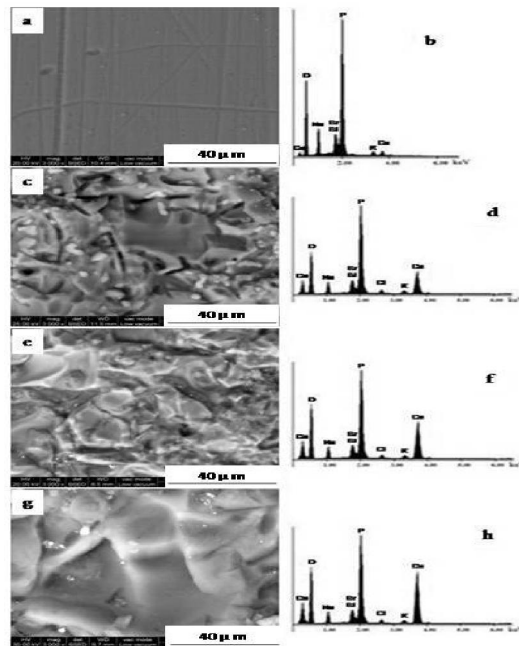


Fig (9): SEM images and the corresponding EDAX spectra of glass GB15: a, b) as-prepared glass, i. e. before soaking in the SBF; c, d) after soaking in the SBF for 7 days; e, f) after soaking in the SBF for 14 days; g, h) after soaking in the SBF for 30 days.

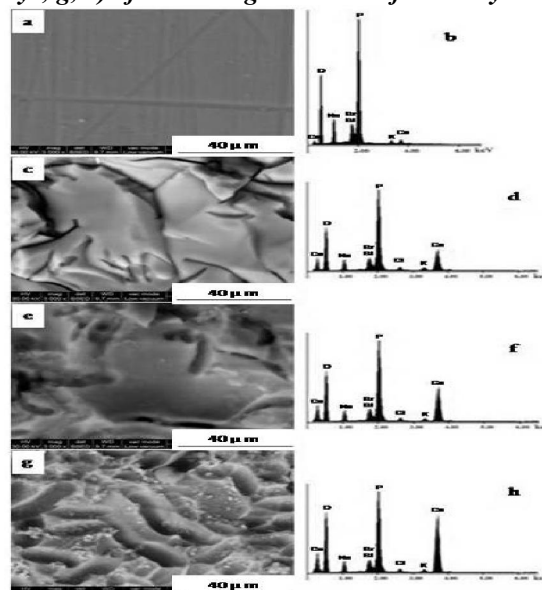


Fig (10): SEM micrographs and the corresponding EDAX spectra of glass GB20: a, b) as-prepared glass, i. e. before soaking in the SBF; c, d) after soaking in the SBF for 7 days; e, f) after soaking in the SBF for 14 days; g, h) after soaking in the SBF for 30 days

Table (2) gave the variation of P, Ca, Si and B ions concentrations in the SBF solution determined by ICP-AES after soaking of the investigated glasses

for 7, 14 and 30 days. Trace amounts of Si-ions that do not exceed 1.2 ppm were detected after 30 days. Very small amounts of B-ions, which reached a maximum of 4.2 ppm, were determined in the SBF solution after the specified time intervals. It can be observed that boron concentration in the SBF, after the same immersion time, very slightly increases with increasing B₂O₃ content in the glass composition. On the other hand, considerable decrease in both of the P and Ca ions in the SBF could be noticed with increasing both of the immersion time and B₂O₃ content in the glass composition. This behavior was graphically represented in Fig. (11).

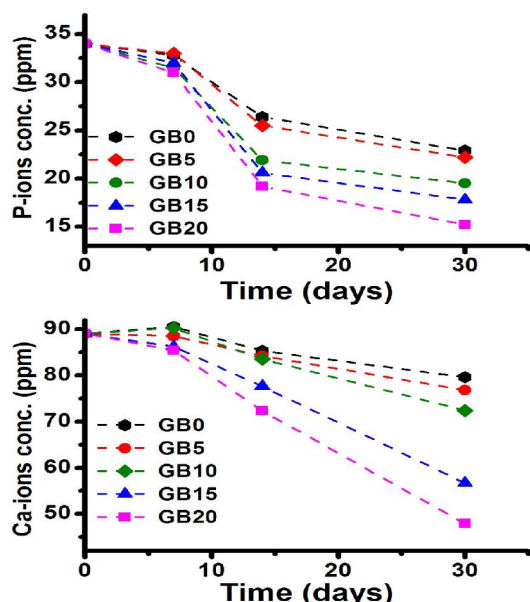


Fig (11). Variation of P- and Ca-ions concentrations in the SBF solution after soaking of the studied glasses for 7, 14 and 30 days.

Table 2. Elemental concentrations in the SBF solution after immersion of the studied glasses for 7, 14 and 30 days.

Glass code	Time (days)	Element concentrations (ppm) ± 0.5			
		Ca	P	Si	B
SBF (standard)		89.05	34.0	0.0	0.0
GB0	7	90.5	32.8	0.2	0.0
	14	85.3	26.4	0.25	0.0
	30	79.6	22.9	0.8	0.0
GB5	7	88.5	33.0	0.0	0.5
	14	84.2	25.5	0.25	0.85
	30	76.8	22.2	0.5	1.2
GB10	7	90.2	31.5	0.3	0.8
	14	83.5	21.9	0.5	1.5
	30	72.4	19.5	0.95	2.2
GB15	7	86.2	32.0	0.5	1.0
	14	77.6	20.6	0.88	2.1
	30	56.7	17.8	1.2	3.0
GB20	7	85.4	31.0	0.25	1.1
	14	72.3	19.2	0.8	2.9
	30	47.9	15.2	0.6	4.2

4. Discussion

In biomaterials research, the in vitro studies, involving dissolution experiments in solutions similar in composition to those present inside the human body (e. g. SBF), have now been recognized as preliminary screening tests on new candidate implant materials, (Roy et al., 2008; Salman et al., 2012). Conventionally, the "bioactivity" (defined as apatite formation) of bioactive glasses is assessed by immersing the glass in SBF, which is a solution saturated in calcium and phosphate, and which mimics the ionic concentrations found in human blood plasma. If the glass results in the formation of apatite in the designated time period, it is conventionally termed bioactive, (Kokubo et al., 1990; Sainz et al., 2010; Mneimne et al., 2011).

The composition of the studied SrO-SiO₂-Na₂O-CaO-B₂O₃-P₂O₅ glass system is an admixture of glass formers, intermediates and modifiers. It is known that B₂O₃ is a well known glass former that participates in the glass network with triangular boron oxygen units mostly condensed as boroxol rings. A part of boron transforms into tetrahedral coordination in the presence of other glass formers and modifiers. It is well known that, among the physical parameters, density and hardness are important parameters to indicate the structural compactness/softening, the change in geometrical configurations, coordination number and cross-linking density of the glass composition, (Rajendran et al., 2000; Azooz et al., 2008; Mohini et al., 2013). Concerning the measured density and microhardness of the as-prepared glasses, the slight decrease of density values can be attributed to the replacement of a heavier component (P₂O₅) by a lighter one (B₂O₃). On the other hand, increasing B₂O₃ content in the glass composition increases the proportions of BO₃ and BO₄ units in the silico-phosphate network which, in turn, increases the cross-linking density of glass structure leading to the relative increase of network compactness and, hence, to the gradual increase of micro-hardness values.

In this study, formation of surface apatite layer was followed using XRD, FTIR, SEM-EDAX and ICP-AES. Experimental XRD patterns confirm the formation of crystalline surface HA layer after 14 and 30 days, while diffraction peaks corresponding to crystalline HA phase were not found in the XRD patterns after 7 days. This may lead to the assumption that, initially after 7 days, either amorphous HA or very poorly crystallized HA or a combination of both was formed on glass surfaces. With the immersion time extended to 14 and 30 days, crystalline HA could be developed on glass surfaces. FTIR performed on both of the virgin surfaces and the immersed ones was used to monitor the formation and growth of the Ca-P layer on glass surfaces by

detecting characteristic vibration modes of the Si-borophosphate network. Interpretation of the obtained FTIR spectra can be performed on basis of previous published articles, (Kim et al., 1989; Jones et al., 2001; Abo-Naf et al., 2004; Rey et al., 2007; Pappas et al., 2008; Duée et al., 2009; Zhao et al., 2009; Fu et al., 2010; Mneimne et al., 2011; Mohini et al., 2013). Concerning the as-prepared glasses, the broad band at 475 cm^{-1} and the shoulder at 515 cm^{-1} are attributed to the bending vibration modes of P—O—P and Si—O—Si bonds, respectively. The shoulder at 710 cm^{-1} could be assigned to the symmetric stretching vibration of P—O—P bond, while that at 810 cm^{-1} to the Si—O—Si symmetric stretching vibration. The broad peaks at 965 and 1090 cm^{-1} are ascribed to the asymmetric stretching vibration of P—O—P bond. The Si—O—Si asymmetric stretching vibration may also interfere in the broad peak at 1090 cm^{-1} . In the spectrum of glass GB0, the broad shoulder at 1210 cm^{-1} is attributed to the P=O bond. Introduction of 5 mol% B_2O_3 in the glass composition, glass GB5, caused shifting of this shoulder to 1225 cm^{-1} due to the interference of B—O stretching vibration of BO_3 triangular structural units in the same spectral range. Systematic increase of B_2O_3 content to 20 mol%, in glasses GB10, GB15 and GB20, results in transformation of this shoulder into medium broad band that is successively shifted to 1270 cm^{-1} , i. e. to a higher wave number, due to the increase of BO_3 groups in the glass structure. Furthermore, diminishing of the band at 965 cm^{-1} with the appearance of a very broad band centered at 940 cm^{-1} in the spectrum of glass GB15 could be ascribed to participation of appreciable proportion of BO_4 tetrahedral units into glass structure. Better resolution of a broad peak at 910 cm^{-1} indicated the increase of BO_4 units in the structure of glass GB20. After soaking the glasses in the SBF for 7 days, the bending vibrations of the silicate and phosphate were shifted to lower wave number values, i. e. 440 and 480 cm^{-1} , with the evolution of a band at 610 cm^{-1} , a shoulder at 560 cm^{-1} and a third signal at 525 cm^{-1} . This range was the most characteristic region for apatitic (PO_4^{3-}) groups and other phosphates. A single band at 610 cm^{-1} suggested the presence of non-apatitic or amorphous calcium phosphate, which was usually taken as an indication of the presence of precursors to apatite. The shoulder at 560 cm^{-1} corresponds to P—O bond vibrations in the PO_4^{3-} tetrahedron and indicated the presence of crystalline calcium phosphates including hydroxyapatite (HAp) and HCA. The third signal at 525 cm^{-1} might be logically attributed to the formation of crystallites of extremely small size. After immersion in the SBF for 14 days, only one pronounced difference could be observed in the spectra of the studied glasses, which

is the development of the shoulder at 560 cm^{-1} into a band whose intensity increased with increasing B_2O_3 in the glass composition. Accordingly, it could be suggested that growth of the crystalline HAp takes place with increasing immersion time, and is also enhanced by increasing B_2O_3 in the glass composition. Extending the immersion time to 30 days further increases the growth of crystalline HAp phase reaching a maximum in case of glass GB20. In general, the characteristic apatitic features present in the FTIR spectra were consistent with the identification of apatite Bragg reflections in the recorded XRD patterns.

After soaking in SBF solution, glass surfaces were strongly modified due to the interfacial chemical reactions between the bioglass and the physiological solution. SEM showed the gradual development of HA layer from a cracked Ca—P rich layer to a porous or microporous layer into a dense, compact and continuous layer completely covered the entire glass surface soaked in SBF for 30 days. Cracks in the calcium phosphate layer probably formed as a result of contractions in the porous hydrated layers when the specimens were dried after being soaked in the SBF, Ho et al., (2010).

It was known that the addition of network modifiers such as Ca^{2+} and Na^+ to bioactive glasses encourages dissolution of the glass by promoting the formation of non-bridging oxygens (NBOs). This promoted changes in surface chemistry which could lead to a precipitated calcium phosphate surface layer that subsequently crystallizes to crystalline HA, Li et al., (2013). Considering the in vitro bioactivity experiments of the present glasses, it could be proposed that glasses release Na^+ ions into the SBF via an exchange with the H^+ (or H_3O^+) ions from the fluid to form P—OH groups on the glass surface. These P—OH groups formed immediately combine with Ca^{2+} ions from the SBF to form an amorphous calcium phosphate and this phase later transforms into bone-like apatite crystals. The apatite formation from the constituent ions is given by the following equation, (Li et al; 1994; Ho et al., 2010):



The apatite nuclei could be initiated once the super-saturation is raised above the critical level necessary for heterogeneous nucleation of apatite. The degree of super-saturation of the soaking solution with respect to apatite increases with the increase of released Na^+ ions. Once the apatite nuclei are formed, they could spontaneously grow by consuming the calcium, phosphate and OH^- ions from the SBF. ICP-AES analysis performed for the SBF revealed significant consumption of both of the calcium and phosphorus ions indicated by the remarkable decrease in their concentrations given in

Table (2) and Fig. (11). The results of the EDS analysis, shown in Figs. (6-10), confirmed these data and supported this mechanism through the marked increase of peak-to-peak ratio of Ca: P with increasing immersion time. In previous studies, (Takadama et al., 2001; Takadama et al., 2002), similar mechanism was proposed for the apatite formation on a sodium silicate glass soaked in SBF through formation of silanol (Si—OH) groups on the glass surface as a result of the ion exchange. These Si—OH groups combined with Ca^{2+} ions from the SBF to form an amorphous calcium silicate on the glass surface. After a long soaking period, this calcium silicate characteristically combines with phosphate ions from the SBF to form an amorphous calcium phosphate which later crystallizes into the HA. In case of the present bio glasses, the mechanism comprising formation of Si—OH groups has only a minor possibility due to the low SiO_2 content (10 mol%) in the glass composition relative to that of P_2O_5 . Factors as chemical composition, surface topography and glass structure are believed to play an important role in the surface interaction of glasses with the surrounding simulated environment and, consequently, significantly affect the in vitro response of bioglasses. Two kinds of glass structures are met: the conventional glasses, containing more bridging oxygen (BO) and presenting a three-dimensional glassy network, and the invert glasses which contained more non-bridging oxygen (NBO) resulting in isolated parts and shorter chains, Duée et al., (2009). Low silica compositions have a more open network structure that facilitates ion exchange with the solution, resulting in faster glass leaching and, in turn, easier precipitation of apatite, Saiz et al., (2002). Leaching and release kinetics are also very important in case of biomaterials used for drug delivery purposes. For instance, advanced drug delivery bioactive hybrid materials were synthesized using the sol-gel processing by Catauro *et al.* 2013 *a and b*.

Overall, it could be observed, from combination of the obtained results, that increasing B_2O_3 content in the present glass composition enhances the bioactivity of the glasses. In previous published articles, (Ning et al., 2007; Manupriya et al., 2009), it was reported that the increase in BO_4 units relatively delays the HA formation on glass surface. Careful inspection of FTIR reflection spectra of the present as-prepared glasses, Fig. (2), indicated that the proportion of BO_3 units increased in the glass structure with increasing B_2O_3 content in the glass composition. BO_3 units with relatively lower cross-linking density could be easily attacked by solution. Therefore, relatively better glass leaching was achieved which might explain the in vitro bioactivity

enhancement trend. It was believed that the present glass system could be a desirable biomaterial for preparing scaffold for tissue engineering.

Conclusions

$\text{SrO-SiO}_2\text{-Na}_2\text{O-CaO-B}_2\text{O}_3\text{-P}_2\text{O}_5$ glasses had been elaborated by the conventional melting method. The SBF immersion experiments showed that the studied glasses exhibited fairly good in vitro bioactivity. The XRD confirmed the formation of a bioactive hydroxyapatite layer on the surface of bioglasses after soaking in SBF solution. The SEM showed a visible and dense apatite layer after 30 days of immersion. The obtained results indicated that increasing B_2O_3 content in the glass composition enhances the bioactivity of the glasses. Evolution and growth of HA layer on glass surfaces have been followed using FTIR, EDS and ICP-AES analyses.

Acknowledgements

The authors are thankful to the scientific research deanship of Northern Border University, Ar'ar, Kingdom of Saudi Arabia, for financial support for funding this project (No. 434-036). The authors are grateful to Prof. Dr. Sherief M. Abo-Naf; Glass Research Dept., National Research Centre (NRC), Egypt; for his valuable scientific consultancy during this project.

References

1. Abo-Naf S. M., Ghoneim N. A., El-Batal H. A., "Preparation and characterization of sol-gel derived glasses in the ternary $\text{Na}_2\text{O-Al}_2\text{O}_3\text{-P}_2\text{O}_5$ system", J. Mater. Sci.: Mater. Electron. 15 (2004) 273-282.
2. Aguiar H., Solla E. L., Serra J., González P., León B., Malz F., Jäger C., "Raman and NMR study of bioactive $\text{Na}_2\text{O-MgO-CaO-P}_2\text{O}_5\text{-SiO}_2$ glasses", J. Non-Cryst. Solids 354 (2008) 5004-5008.
3. Aguiar H., Solla E. L., Serra J., González P., León B., Almeida N., Cachinho S., Davim E. J. C., Correia R., Oliveira J. M., Fernandes M. H. V., "Orthophosphate nanostructures in $\text{SiO}_2\text{-P}_2\text{O}_5\text{-CaO-Na}_2\text{O-MgO}$ bioactive glasses", J. Non-Cryst. Solids 354 (2008) 4075-4080.
4. Azooz M. A., Abou Aiad T. H. M., Elbatal F. H., ElTabii G., "Characterization of bioactivity in transition metal doped-borosilicate glasses by infrared reflection and dielectric studies", Ind. J. Pure Appl. Phys. 46 (2008) 880-888.
5. Catauro M., Papale F., Roviello G., Ferone C., Bollino F., Trifuoggi M., Aurilio C., "Synthesis of SiO_2 and CaO rich calcium silicate systems via sol-gel process: Bioactivity, biocompatibility and drug delivery tests", J.

- Biomed. Mater. Res. A 2013, doi: 10. 1002/jbm.a. 34978 Online.
6. Catauro M., Bollino F., Papale F., Pacifico S., Galasso S., Ferrara C., Mustarelli P., "Synthesis of zirconia/polyethylene glycol hybrid materials by sol-gel processing and connections between structure and release kinetic of indomethacin", Drug Deliv. 2013, doi: 10. 3109/10717544. 2013. 865816 Online.
 7. Day D. E., White J. E., Brown R. F., McMenamin K. D., "Transformation of borate glasses into biologically useful materials", Glass Technol. 44 (2003) 75-81.
 8. Ducheyne P., Qiu Q., "Bioactive ceramics: the effect of surface reactivity on bone formation and bone cell function", Biomaterials 20 (1999) 2287-2303.
 9. Ducheyne P., "Bioglass coatings and bioglass composites as implant materials", J. Biomed. Mater. Res. 19 (1985) 273-291.
 10. Duée C., Désanglois F., Lebecq I., Moreau G., Leriche A., Follet-Houttemane C., "Mixture designs applied to glass bioactivity evaluation in the Si-Ca-Na system", J. Non-Cryst. Solids 355 (2009) 943-950.
 11. Fu H., Rahaman M. N., Day D. E., Huang W., "Effect of pyrophosphate ions on the conversion of calcium-lithium-borate glass to hydroxyapatite in aqueous phosphate solution", J. Mater. Sci.: Mater. Med. 21 (2010) 2733-2741.
 12. Jones J. R., Sepulveda P., Hench L. L., "Dose-dependent behavior of bioactive glass dissolution", J. Biomed. Mater. Res. 58 (2001) 720-726.
 13. Han X., Du M., Ma Y., Day D. E., "Evaluation of hydroxyapatite microspheres made from a borate glass to separate protein mixtures", J. Mater. Sci. 43 (2008) 5618-5625.
 14. Hench L. L., "Bioceramics", J. Am. Ceram. Soc. 81 (1998) 1705-1728
 15. Hench L. L., Splinter R. J., Allen W. C., Greenlee T. K., "Bonding mechanisms at the interface of ceramic prosthetic materials", J. Biomed. Mater. Res. 2 (1971) 117-141.
 16. Ho W., Lai C., Hsu H., Wu S., "Surface modification of a Ti-7. 5Mo alloy using NaOH treatment and Bioglass® coating", J. Mater. Sci.: Mater. Med. 21 (2010) 1479-1488.
 17. Kokubo T., Kushitani H., Sakka S., Kitsugi T., Yamamuro T., "Solution able to reproduce in vivo surface-structure changes in bioactive glass-ceramics A-W", J. Biomed. Mater. Res. 24 (1990) 721-734.
 18. Kokubo T., Takadama H., "How useful is SBF in predicting in vivo bone bioactivity?", Biomaterials 27 (2006) 2907-2915.
 19. Kim C. Y., Clark A. E., Hench L. L., "Early stages of calcium-phosphate layer formation in bioglasses", J. Non-Cryst. Solids 113 (1989) 195-202.
 20. Li Y., Coughlan A., Laffir F. R., Pradhan D., Mellott N. P., Wren A. W., "Investigating the mechanical durability of bioactive glasses as a function of structure, solubility and incubation time", J. Non-Cryst. Solids 380 (2013) 25-34.
 21. Li P., Kangasniemi I., de Groot K., Kokubo T., "Bone-like hydroxyapatite induction by a gel-derived titania on a titanium substrate", J. Am. Ceram. Soc. 5 (1994) 1307-1312.
 22. Manupriya, K. S. Thind, K. Singh, V. Kumar, G. Sharma, D. P. Singh, D. Singh, "Compositional dependence of in-vitro bioactivity in sodium calcium borate glasses", J. Phys. Chem. Solids 70 (2009) 1137-1141.
 23. Marikani, A. Maheswaran, M. Premanathan, L. Amalraj, "Synthesis and characterization of calcium phosphate based bioactive quaternary P₂O₅-CaO-Na₂O-K₂O glasses", J. Non-Cryst. Solids 354 (2008) 3929-3934.
 24. Mneimne M., Hill R. G., Bushby A. J., Brauer D. S., "High phosphate content significantly increases apatite formation of fluoride-containing bioactive glasses", Acta Biomater. 7 (2011) 1827-1834.
 25. Mohini G. J., Krishnamacharyulu N., Baskaran G. S., Rao P. V., Veeraiah N., "Studies on influence of aluminum ions on the bioactivity of B₂O₃-SiO₂-P₂O₅-Na₂O-CaO glass system by means of spectroscopic studies", Appl. Surface Sci. 287 (2013) 46-53.
 26. Ning J., Yao A., Wang D., Huang W., Fu H., Liu X., Jiang X., Zhang X., "Synthesis and in vitro bioactivity of a borate-based bioglass", Mater. Lett. 61 (2007) 5223-5226.
 27. Pappas G. S., Liatsi P., Kartsonakis I. A., Danilidis I., Kordas G., "Synthesis and characterization of new SiO₂-CaO hollow nanospheres by sol-gel method: Bioactivity of the new system", J. Non-Cryst. Solids 354 (2008) 755-760.
 28. Rajendran V., Palanivelu N., Modak D. K., Chaudhuri B. K., "Ultrasonic investigation on ferroelectric BaTiO₃doped 80V₂O₅-20PbO oxide glasses", Physica Status Solidi A 180 (2000) 467-477.
 29. Renghini C., Giuliani A., Mazzoni S., Brun F., Larsson E., Bairo F., Vitale-Brovarone C., "Microstructural characterization and *in vitro* bioactivity of porous glass-ceramic scaffolds for

- bone regeneration by synchrotron radiation X-ray microtomography", *J. Eur. Ceram. Soc.* 33 (2013) 1553-1565.
30. Rezwan K., Chen Q. Z., Blaker J. J., Boccaccini A. R., "Biodegradable and bioactive porous polymer/inorganic composite scaffolds for bone tissue engineering", *Biomaterials* 27 (2006) 3413-3431.
 31. Rey C., Combes C., Drouet C., Lebugle A., Sfihi H., Barroug A., "Nanocrystalline apatites in biological systems: characterization, structure and properties", *Materialwiss. Werkst.* 38 (2007) 996-1002.
 32. Richard M. N. C., "Bioactive behavior of a borate glass", M. S. Thesis, University of Missouri-Rolla, (2000) p. 68.
 33. Roy S., Basu B., "In vitro dissolution behavior of SiO₂-MgO-Al₂O₃-K₂O-B₂O₃-F glass-ceramic system", *J. Mater. Sci.: Mater. Med.* 19 (2008) 3123-3133.
 34. Salman S. M., Salama S. N., Abo-Mosallam H. A., "The role of strontium and potassium on crystallization and bioactivity of Na₂O-CaO-P₂O₅-SiO₂ glasses", *Ceram. Int.* 38 (2012) 55-63.
 35. Sainz M. A., Pena P., Serena S., Caballero A., "Influence of design on bioactivity of novel CaSiO₃-CaMg(SiO₃)₂ bioceramics: in vitro simulated body fluid test and thermodynamic simulation", *Acta Biomater.* 6 (2010) 2797-2807.
 36. Saiz E., Goldman M., Gomez-Vega J. M., Tomsia A. P., Marshall G. W., Marshall S. J., "In vitro behavior of silicate glass coatings on Ti6Al4V", *Biomaterials* 23 (2002) 3749-3756.
 37. Siqueira R. L., Zanotto E. D., "The influence of phosphorus precursors on the synthesis and bioactivity of SiO₂-CaO-P₂O₅ sol-gel glasses and glass-ceramics", *J. Mater. Sci.: Mater. Med.* 24 (2013) 365-379.
 38. Takadama H., Kim H. M., Kokubo T., Nakamura T., "Mechanism of biomineralization of apatite on a sodium silicate glass: TEM-EDX study in vitro", *Chem. Mater.* 13 (2001) 1108-1113.
 39. Takadama H., Kim H. M., Kokubo T., Nakamura T., "X-ray photoelectron spectroscopy study on the process of apatite formation on a sodium silicate glass in simulated body fluid", *J. Am. Ceram. Soc.* 85 (2002) 1933-1936.
 40. Yao A., Wang D., Huang W., Fu Q., Rahaman M. N., Day D. E., "In vitro bioactive characteristics of borate-based glasses with controllable degradation behavior", *J. Am. Ceram. Soc.* 90 (2007) 303-306.
 41. Zhao D., Huang W., Rahaman M. N., Day D. E., Wang D., "Mechanism for converting Al₂O₃-containing borate glass to hydroxyapatite in aqueous phosphate solution", *Acta Biomater.* 5 (2009) 1265-1273.

7/19/2014